AD-A132 014 TECHNIQUES FOR LOCATING A REMOTE HF TRANSMITTER FROM SINGLE-SITE MEASUREMENTS(U) NAVAL RESEARCH LAB WASHINGTON DC M H REILLY 11 AUG 83 NRL-MR-5145 1/1

UNCLASSIFIED F/G 17/3 NL

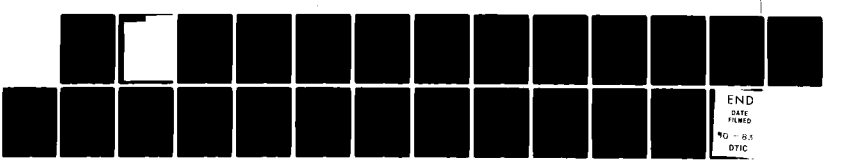

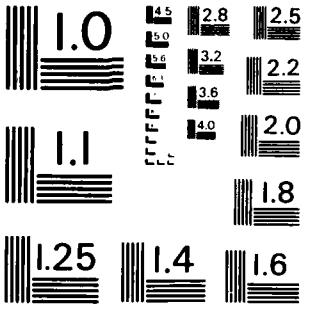

MICROCOPY RESOLUTION TEST CHART
NATIONAL BUREAU OF STANDARDS - 1963 - A

SECURITY CLASSIFICATION OF THIS PAGE (When Data Entered)

REPORT DOCUMENTATION PAGE	READ INSTRUCTIONS BEFORE COMPLETING FORM
1 REPORT NUMBER: NRL Memorandum Report 5145	2 GOVT ACCESSION NO.: AD-A132 014
3 RECIPIENT'S CATALOG NUMBER:	
4 TITLE (and Subtitle): TECHNIQUES FOR LOCATING A REMOTE HF TRANSMITTER FROM SINGLE-SITE MEASUREMENTS	5 TYPE OF REPORT & PERIOD COVERED: Interim report on a continuing NRL problem.
	6 PERFORMING ORG. REPORT NUMBER:
7 AUTHOR(s): M.H. Reilly	8 CONTRACT OR GRANT NUMBER(s):
9 PERFORMING ORGANIZATION NAME AND ADDRESS: Naval Research Laboratory, Washington, DC 20375	10 PROGRAM ELEMENT, PROJECT, TASK AREA & WORK UNIT NUMBERS: 41-0661-0-3
11 CONTROLLING OFFICE NAME AND ADDRESS:	12 REPORT DATE: August 11, 1983
	13 NUMBER OF PAGES: 23
14 MONITORING AGENCY NAME & ADDRESS(if different from Controlling Office): U.S. Army Signal Warfare Laboratory, Vint Hill Farms Station, Warrenton, VA 22186	15 SECURITY CLASS. (of this report): UNCLASSIFIED
	15a DECLASSIFICATION/DOWNGRADING SCHEDULE:

16 DISTRIBUTION STATEMENT (of this Report)

Approved for public release; distribution unlimited.

17 DISTRIBUTION STATEMENT (of the abstract entered in Block 20, if different from Report)

18 SUPPLEMENTARY NOTES

19 KEY WORDS (Continue on reverse side if necessary and identify by block number)

Radio direction finding
Single-site measurements
Curved ionosphere effects
DF techniques
Breit-Tuve and Martyn theorem generalizations

20 ABSTRACT (Continue on reverse side if necessary and identify by block number)

Techniques are developed for the location of a remote HF transmitter from single-site DF measurements on the incoming wavefront, coupled with ionospheric data. A simple method is detailed, which utilizes the Breit-Tuve and Martyn equivalent path theorems in a flat ionosphere approximation. It is shown to break down in this application only for high elevation angles and frequencies. Curved ionosphere —

(Continues)

DD FORM 1 JAN 73 1473 EDITION OF 1 NOV 65 IS OBSOLETE
S/N 0102-014-6601

SECURITY CLASSIFICATION OF THIS PAGE (When Data Entered)

20. ABSTRACT (Continued)

generalizations of these theorems are developed to remove this breakdown. These generalizations are found to be remarkably accurate within the context of the neglect of magnetic field and non-spherical ionosphere effects, and are shown to be applicable to the present problem.

CONTENTS

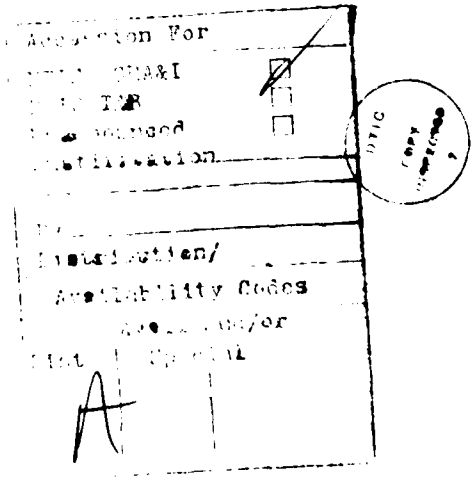

TECHNIQUES FOR LOCATING A REMOTE HF TRANSMITTER FROM SINGLE-SITE MEASUREMENTS

1. Introduction

For answering a ship's distress call, and for similar situations, it is important to be able to convert measurements at a single site to a rapid determination of the position of a remote HF transmitter. The transmitter may be located several hundred kilometers and one or more ionospheric reflections away from the receiver. Radio direction finding (DF) measurements [Gething, 1978] can provide the frequency, azimuth angle, and elevation angle of the incoming wavefront. Information about the ionosphere - e.g., as obtained from sounder measurements or from a statistical model - is then fed into propagation calculations to determine the position of the transmitter. It is this latter aspect of the problem which is treated here.

Ionosonde measurements typically provide ionospheric information at a given location. As a first approximation, the ionosphere could be assumed to be constant along the raypath. Calculations are greatly simplified, and a good initial estimate of transmitter position is often obtained. A constant ionosphere is assumed here. The incorporation of ionospheric tilt effects [Gething, 1978] is currently being investigated.

Magnetic effects are also neglected here. Again, calculations of transmitter position are greatly simplified, and a good first estimate is obtained in a timely fashion. Indeed, typical DF measurements do not identify the polarization of the incoming ray. Hence, its ionospheric history as extraordinary (X) or ordinary(O) mode propagation is typically unknown. Gething [1978] points out that no-field transmitter fixes are intermediate between those for O- and X- mode ray traces, which can differ by 5-10%.

The propagation calculation technique depends on the type of ionospheric information which is given. If the complete density vs. true height profile has been determined - e.g., through computer-processing of ionograms - the position of the HF transmitter can be computed by a direct scattering calculation, as discussed in Section 2, or by a computer ray-tracing program. When microcomputers are involved the direct scattering type of calculation can be appreciably more time-efficient. When only the virtual height profile is available, which is given by a vertical incidence ionogram, a simple method of processing this information can be used which employs the Breit-Tuve and Martyn theorems [e.g., Budden, 1966] appropriate for curved earth and flat ionosphere. This method is discussed in Section 3. The generalizations of these theorems for a curved ionosphere and a method based on them is given in Section 4. Finally, the results are discussed in Section 5.

Manuscript approved May 26, 1983.

2. IONOSPHERIC DENSITY PROFILE KNOWN

If the ionospheric electron density vs. height profile is known, and the frequency, elevation angle, and azimuth angle of the incoming ray have been specified by DF measurements, the HF transmitter position can be determined by computer ray-tracing. This approach is well known, but is often time-consuming on a microcomputer. Alternatively, a direct scattering calculation is relatively fast and accurate for a constant ionosphere (profile independent of range). Such calculations assume an analytic fit to the electron density which is integrable in the expressions for range, group-path length, and phase-path length. A summary is given by Gething [1978]. A particular technique that I have found useful employs the analytic fit of deVoogt [1953], along with Lagrangian interpolation of tabulated density values. It is summarized here for convenience, and to establish the notation of subsequent sections.

The index of refraction of a collisionless plasma is

$$\mu^2 = 1 - f_N^2(R)/f^2 \tag{1}$$

where f is the radio frequency, and $f_N(R)$ is the height-dependent plasma frequency, which is defined in terms of the electron density N by (MKS units)

$$4\pi^2 f_N^2(R) \equiv N(R)e^2/m\epsilon_0 \tag{2}$$

The path of the ray and some relevant notation are indicated in Fig. 1. The path of the ray satisfies a spherical Snell's Law [e.g., Freehafer, 1951], given by (cf. Fig. 1)

$$\mu R \cos\beta = \text{const.} = R_0 \cos\beta_0 \tag{3}$$

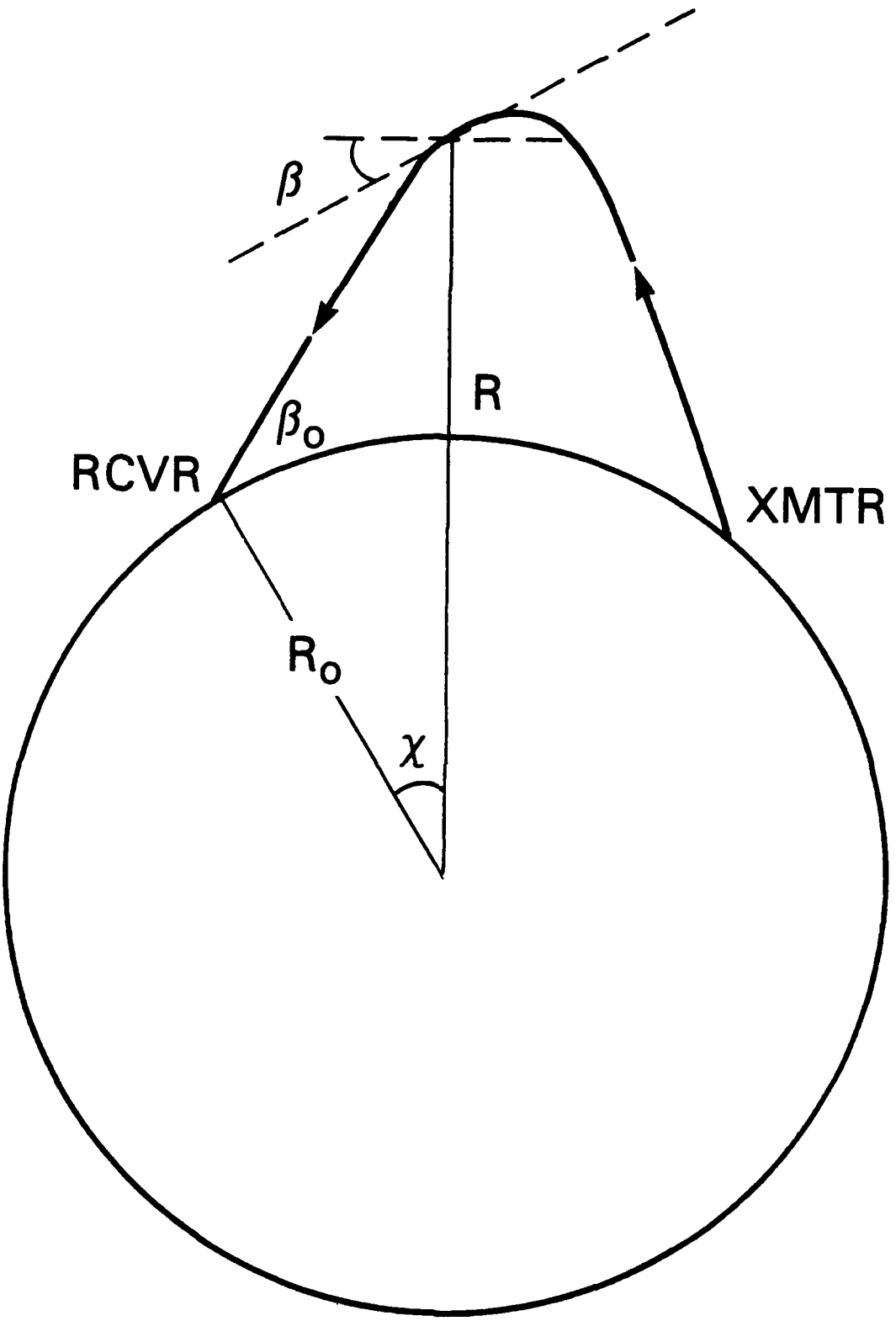

Fig. 1 — Ray path geometry (cf. Sec. 2)

A raypath element traces out a ground range

$$d D = R_0 \, d\chi = (R_0/R) \, dR \cot \beta \tag{4}$$

Hence, χ is interchangeable with D, and is from (3)

$$\chi/2 = R_0 \cos \beta_0 \int_{R_0}^{R_t} \frac{dR}{R \sqrt{\mu^2 R^2 - R_0^2 \cos^2 \beta_0}} \tag{5}$$

where R_t refers to the radius of reflection of the ray. At this point $\beta = 0$ and the denominator of the integrand vanishes. The starting point is a set of values f_{Ni} at discrete altitude points H_i or radius points R_i where $R_i = R_0 + H_i$ $(i = 1,2,-----, 2N + 1)$. In regions of the R-domain in (5) where $f_N^2 = 0$, i.e., a free-space propagation region,

$$\chi_f/2 = \cos^{-1} (R_0 \cos \beta_0 / R) \quad , \tag{6}$$

which is to be evaluated between limits of the free-space region. In the ionospheric region of the R-domain, where the electron density is non-vanishing, the contribution to (5) can be evaluated by fitting a parabola (deVoogt, 1953) to an adjacent triad of values of $R_i^2 f_{Ni}^2$. Then the radicand in Eq. (5) in the associated radius interval can be written in the form

$$\mu^2 R^2 - R_0^2 \cos^2 \beta_0 = A + BR + CR^2 \tag{7}$$

in the associated radius interval $P \leqq R \leqq Q$. A different set of coefficients A,B,C,P, and Q is associated with each triad of mesh points. The coefficients for the J'th such triad involve the mesh points at 2J-1, 2J, and 2J+1 (J=1,2,---,N). For example, $P(J) = R_{2J-1}$ and $Q(J) = R_{2J+1}$. This procedure is specified for a triad of points in Appendix A, where the range contribution from these points is indicated [see (A8)]. The total ionospheric contribution involves a sum over J of such range contributions.

Appendix A also includes an evaluation of group path length, which will be used in a later section. The contribution to group path length from a raypath length element ds is

$$d P' = \frac{c \, ds}{d\omega/dk} = ds \, \frac{d}{df} (\mu f) = \frac{ds}{\mu} \tag{8}$$

Hence, from (3) and Figure 1

$$P'/2 = \int_{R_0}^{R_x} \frac{dR}{\mu \sin\beta} = \int_{R_0}^{R_x} \frac{R\,dR}{\sqrt{\mu^2 R^2 - R_0^2 \cos^2\beta_0}} \tag{9}$$

For a range of R where plasma density vanishes,

$$P_f'/2 = \sqrt{R^2 - R_0^2 \cos^2\beta_0} \tag{10}$$

which is to be evaluated between limits of the free-space region. The ionospheric contribution is facilitated by (7) and is again the summation over J of contributions from triads of adjacent points, as indicated in Appendix A [cf (A9)]. The above procedure is easily implemented on the computer.

3. VIRTUAL HEIGHT PROFILE GIVEN - A SIMPLE METHOD

In case vertical ionosonde measurements are taken, or oblique ionosonde measurements are converted to this form, the data available consists of a plot of vertical time delay τ of a pulse vs frequency f. Virtual height h' is defined as

$$h'(f) = c\,\tau(f)/2 \tag{11}$$

It is interesting that a simple and quite accurate method exists which uses this data in conjunction with Breit and Tuve's theorem and Martyn's theorem for a flat ionosphere [Budden, 1966], although the earth's curvature is otherwise taken into account. The idea is that, even though the total range may exceed 1000 km, only a small part of the raypath occurs in the ionospheric region in many instances. Hence, the earth's curvature can be neglected for the ionospheric portion of the raypath, in which case the above theorems can be used.

The algorithm for determining range from measured frequency f and elevation angle β_0 is described next with reference to Figure 2:

---------- ALGORITHM 1----------

(1) Guess a range D, and $\chi = D/2R_0$
(2) Calculate $i = \pi/2 - \beta_0 - \chi$ and $C = \cos i$
(3) Determine P' from Martyn's equivalent path theorem

$$P'/2 = (h'(fC) + \Delta)/C$$

where

$$\Delta = R_0(1 - \cos\chi)$$

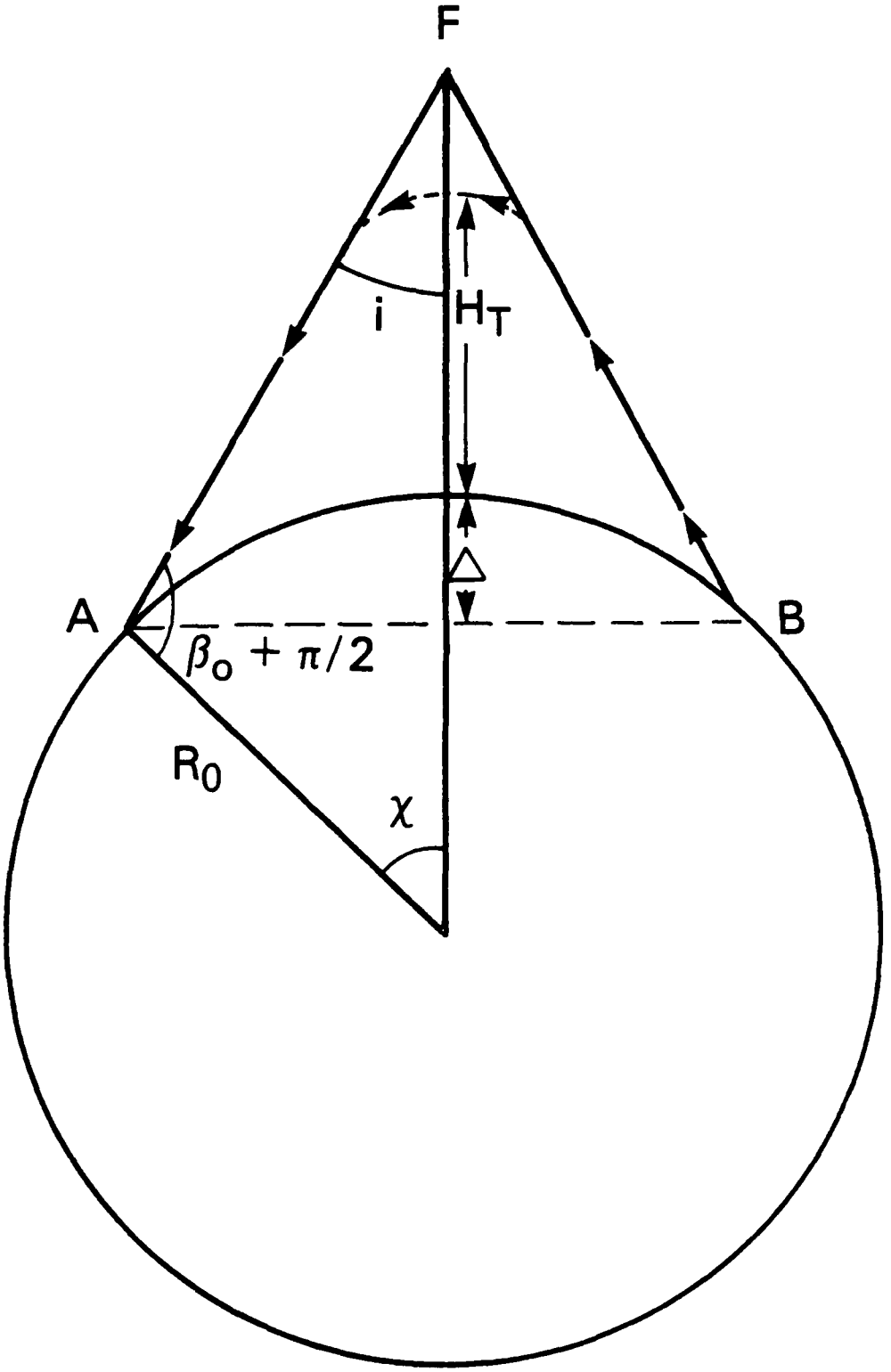

Fig. 2 — Illustration of notation (cf. Sec's 3,4)

(4) Determine a new D from the Breit-Tuve theorem. The law of sines gives

$$P'/2 = AF = R_o \sin\chi / \cos(\beta_o + \chi)$$

which can be inverted to give

$$\chi = \tan^{-1}\left(\frac{(P'/2)\cos\beta_o}{R_o + (P'/2)\sin\beta_o} \right)$$

(5) Compare the new value of $D = 2 R_o\chi$ with the old value to see if it is within tolerance. If so, terminate the calculation. If not, go back to (2) and repeat the ensuing steps with the value of χ just calculated in (4).

The preceding algorithm is tested for the case of a simple F-layer. The layer is modeled as a simple "quasi-parabola", which has the form [Croft and Hoogasian, 1968]

$$f_N^2(R) = f_p^2 \left[1 - \frac{(R-R_m)^2 R_b^2}{y_m^2 R^2} \right] \qquad (12)$$

where R_b is the radius of the bottom of the layer, R_m is the radius of the layer maximum, and y_m is its semi-thickness ($R_b = R_m - y_m$). It will be noted that for layers of this form, the form of (7) is exact, and the relevant integrals are thus easily calculated. The parameters of the layer used for calculations are f_p = 10 MHz, $H_b = R_b - R_o$ = 230 km, and y_m = 120 km. The calculated virtual height profile is shown in Figure 3, and the results of the preceding computerized algorithm are shown in Table 1. Ranges are carried out to two decimal places for the purpose of comparison of the DF range values with the exact range values. The exact values are calculated for this simple case, using the results of the preceding section and Appendix 1.

It is seen from Table 1 that the flat ionosphere approximation, inherent in the algorithm, works very well for small elevation angles and for frequencies beneath f_p. Errors for the 11 MHz ($f > f_p$) case do not approach 1% until the elevation angle exceeds 50°. The portion of the raypath in the ionosphere becomes long enough at this point, that the flat ionosphere approximation begins to break down. Sensitivty to the approximation also increases for the large elevation angles, where the large, rapidly varying (with frequency) values of virtual height come into play. The 11 MHz ray escapes the layer altogether for elevation angles greater than 63.93°. The elevation angles greater than 60° correspond to Pedersen or "high" ray propagation [Budden, 1966]. It is especially for these rays that the preceding algorithm breaks down.

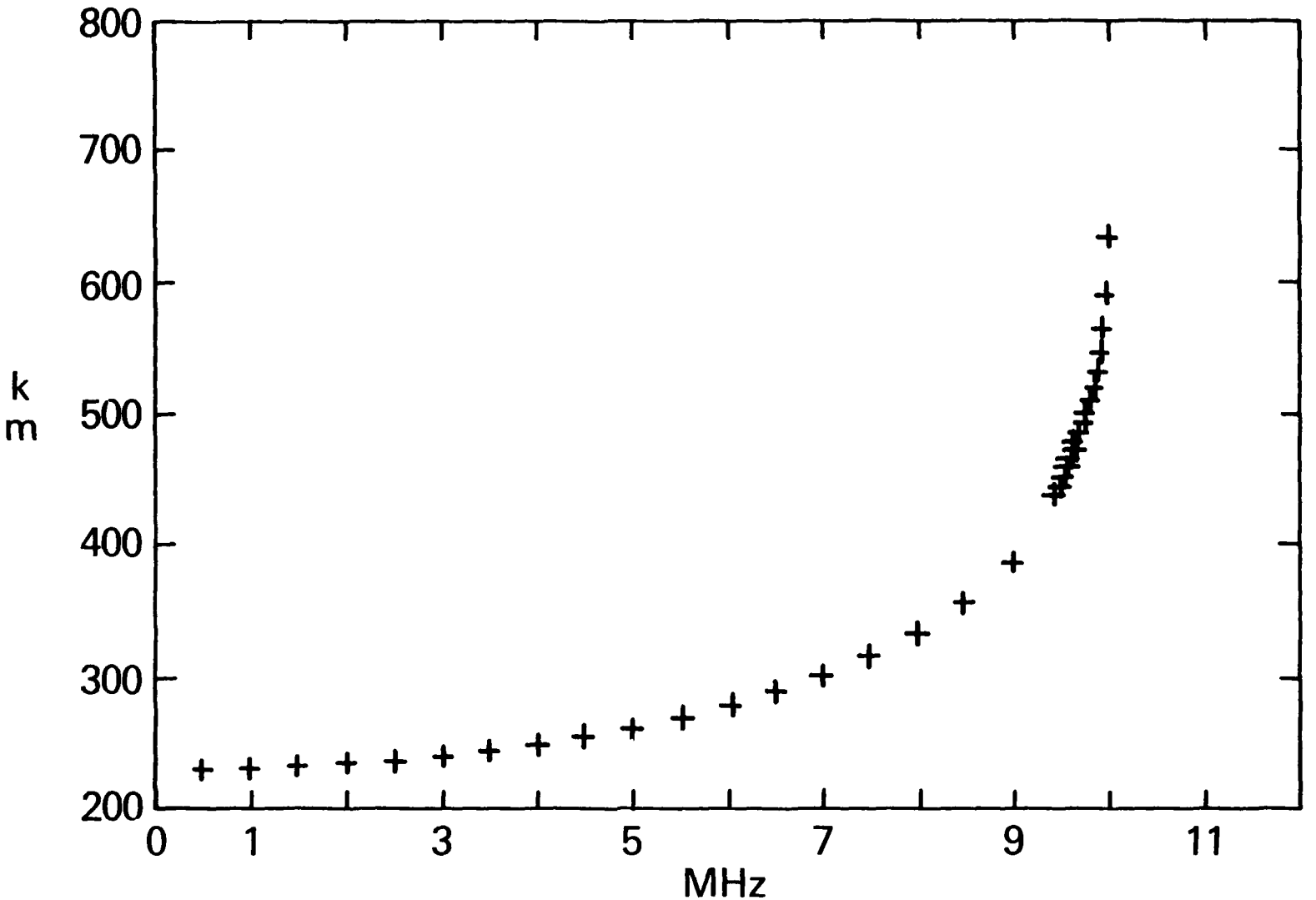

Fig. 3 — Virtual height profile of a quasiparabolic F-layer (cf. Sec. 3)

TABLE 1. DF RANGE DETERMINATION FROM VIRTUAL HEIGHT PROFILES

(cf. Sec. 3)

FREQ. (MHz)	El. Angle (°)	DF RANGE (km)	EXACT RANGE (km)	ERROR (%)
11	10	1889.75	1888.82	.05
	15	1482.18	1481.11	.07
	20	1210.04	1208.81	.10
	25	1020.91	1019.56	.13
	35	779.89	778.28	.21
	45	632.10	630.13	.31
	55	535.32	530.38	.93
	60	513.07	504.12	1.78
	61	519.31	504.89	2.86
	62	544.50	511.64	6.42
8	10	1846.90	1846.67	.01
	15	1432.07	1431.81	.02
	20	1151.30	1151.02	.02
	30	805.52	805.24	.03
	40	598.65	598.45	.03
	50	451.97	451.88	.02
	60	331.39	331.49	.03
	70	220.33	220.53	.09
	80	110.69	110.84	.14

It is worth noting that convergence of the preceding algorithm is rapid, even if the starting guess for the range is grossly inaccurate. For example, for the 11 MHz ray and an elevation angle of 5°, if one initially guesses a range of 200 km, the calculated range is within about 1% of its final value of 2513.6 km after three iterations. Convergence to six significant figures and two decimal places is obtained after seven iterations.

4. IMPROVEMENTS FROM CURVED IONOSPHERE GENERALIZATIONS

The algorithms of the preceding section can be improved at high elevation angles by generalizing the Breit-Tuve and Martyn equivalent path theorems beyond the flat ionosphere approximation. The Breit-Tuve theorem relates group-path length to χ ($= D/R_o$) in Figure 1. From (3) and (8)

$$dP' = \frac{ds}{\mu} = \frac{R\,d\chi}{\mu \cos\beta} = \frac{R^2}{R_o \cos\beta_o}\,d\chi \qquad (13)$$

The ray follows a straight line in free space up to the ionosphere. If the curvature of the ionosphere could be neglected, then the Breit-Tuve theorem would allow for the calculation of group path length, much as if the ray continues its straight-line path in the ionosphere, unaffected by it, up to F in Figure 2. If this were true, the radius R could be deduced from the law of sines in Figure 1 as

$$R = R_o \cos\beta_o \,/\, \cos(\beta_o + \chi) \qquad (14)$$

Substitution of this equation in (13) and integration over the total range does yield the curved-earth, flat ionosphere Breit-Tuve theorem used in step (4) of the algorithm of the preceding section. In the ionosphere, however, the ray actually follows the dashed path shown in Figure 2, where it gets reflected at the radius $R_t = R_o + H_t$. The improvement suggested here is to approximate R in (13) by (14) for $0 \leq R \leq R_t$, where R_t corresponds to χ_t, and then to set $R = R_t$ for $\chi_t \leq \chi \leq \chi_D$, where χ_D corresponds to the total range. Hence, one obtains from the integral of (13) over χ from 0 to χ_D ($= D/2R_o$)

$$P'/2 = (R_t / R_o \cos\beta_o)\left[R_o \sin\chi_t + R_t(\chi_D - \chi_t)\right] \qquad (15)$$

where,

$$\chi_t = -\beta_o + \cos^{-1}(R_o \cos\beta_o / R_t)\,,$$

and R_t, the reflection radius, is obtained from

$$f_N^2(R_t)/f^2 = 1 - (R_o \cos\beta_o / R_t)^2 \qquad (16)$$

The price paid for this generalization of the Breit-Tuve theorem is loss of simplicity. The details of the ionospheric true-height density profile now creep into the result, because of the dependence of R_t on f.
In Table 2, various relations between P' and D are tested for the quasiparabolic F-layer used for Table 1. D is computed exactly, and P' is computed from the relation being tested. The first and second columns give frequency f and elevation angle β_0. The third column gives exact values of group path length P', which were calculated along with the exact values of range D given in Table 1. The fourth column is the Breit-Tuve result for P', ie., PBT', which relation was used in the algorithm of Sec. 3. The fifth column is the value of P' from (15), ie., PR1'. The sixth column gives P' from the Maliphant and Muldrew [1963] relation, i.e., PMM'. This relation was used by Smith [1970] in his method for extracting ionospheric profiles from oblique incidence ionograms. The relation can be simply obtained from (15) by replacing the square-bracketed term there by $R_0 x_D$.

It is seen from Table 2 that PBT' is accurate for all but the highest elevation angles for $f > f_p$ (= 10 MHz). It is also seen that PR1' is remarkably accurate for all the elevation angles listed. The errors for PMM' are largest in Table 2, but they are only in the range 1-2% for high values of elevation angle when $f > f_p$.

Martyn's equivalent path theorem relates group path length for oblique propagation to virtual height for the vertical path associated with the same reflection altitude. A generalization of this relationship beyond the flat ionosphere approximation in step (3) of the algorithm in Sec. 3 is derived in Appendix B. For greater generality, an E-layer is included in the analysis along with the F-layer. Just as with (15), the application of the results requires some knowledge of the ionospheric density-true height profile, which can be obtained from processing the virtual height profile. The reflection height $H_t = R_t - R_0$ is found from the solution of (16). Then the solution for the equivalent vertical incidence frequency f_v is given by

$$f_v = f \sqrt{1 - (R_0 \cos\beta_0 / R_t)^2} \tag{17}$$

It will now be useful to define a density profile parameter

$$K(f, \beta_0, R) \equiv 2 \Big/ \left| \frac{1}{f^2} \frac{d f_N^2(R)}{dR} - \frac{2}{R} \left(\frac{R_0 \cos\beta_0}{R} \right)^2 \right| \tag{18}$$

which involves the slope of the density at R [cf. (2)]. In terms of this parameter it is found in Appendix B that

$$P'/2 \approx \sqrt{R_{BF}^2 - R_0^2 \cos^2\beta_0} - R_0 \sin\beta_0 + \Delta_E(f, \beta_0) + \sqrt{2(R_x - R_{BF}) K(f, \beta_0, R_x)} \tag{19}$$

TABLE 2. COMPARISON OF GROUP PATH LENGTHS CALCULATED FROM THREE BREIT-TUVE TYPES OF RELATIONS (cf. Sec 4)

FREQ. (MHz)	El. ANGLE (°)	EX CT P' (km)	PBT' (km)	PR1' (km)	PMM' (km)
11	10	1984.30	1984.38	1984.32	1989.38
	15	1589.92	1590.04	1589.95	1591.10
	20	1336.35	1336.55	1336.40	1335.60
	25	1170.83	1171.16	1170.91	1168.85
	35	993.03	993.85	993.22	989.10
	45	936.40	938.31	936.81	930.16
	55	978.85	983.73	979.78	968.60
	60	1073.50	1083.01	1075.05	1058.74
	61	1110.72	1122.23	1112.48	1094.29
	62	1164.85	1179.53	1166.92	1146.02
8	10	1938.26	1938.28	1938.26	1943.45
	15	1534.97	1535.00	1534.98	1537.02
	20	1270.06	1270.10	1270.07	1270.45
	30	966.24	966.35	966.27	965.14
	40	813.65	813.89	813.71	811.72
	50	733.92	734.34	734.02	731.28
	60	693.75	694.42	693.91	690.46
	70	676.09	677.04	676.30	672.19
	80	670.25	671.43	670.51	665.92

where $\Delta_E(f,B_o)$ is the contribution of E-layer retardation (=0 for no E-layer). Δ_E is given by (B2) and (B4) of Appendix B. It can be evaluated for typical E-layer distributions by fitting a quasiparabola to the observed E-layer profile, and then using the formulae of Sec. 2 and Appendix A. This quasiparabola can even be directly obtained from the virtual height profile. Its contribution will often be insignificant in HF-DF applications. The parameter R_{BF} corresponds roughly to the bottom of the F-layer, but, more accurately, it contains the dependence on $h'(f_v)$ through

$$H_{BF} = R_{BF} - R_o = \hat{h}_v - K_v + K_v \sqrt{1 - 2(\hat{h}_v - H_t)/K_v} \qquad (20)$$

where

$$\hat{h}_v \equiv h'(f_v) - \Delta_E(f_v, \pi/2) \qquad (21)$$

and

$$K_v \equiv K(f_v, \pi/2, R_t) \qquad (22)$$

Equations (16-22) constitute the proposed generalization of Martyn's equivalent path theorem. It is evaluated in Table 3 as PR2' for the quasiparabolic F-layer case of Tables 1 and 2, and is compared with the flat ionosphere approximation in step (3) of the algorithm in Sec. 3, denoted by PM' in Table 3. The rest of the parameters are identical with those of Table 2.

From Table 3 it is seen that the flat ionosphere Martyn's theorem PM' values are quite accurate for the smaller elevation angles. Beyond 50° the errors increase with elevation angle, approaching several percent for the Pedersen rays. This is similar to the situation in Table 1. Associated errors in Table 2 for the flat ionosphere Breit-Tuve theorem are substantially less for high elevation angles. It therefore appears that most of the error at high elevation angles in the algorithm of Sec. 3 arises from the use of Martyn's theorem there. By contrast, it is seen that the generalization PR2' is extremely accurate for all elevation angles. This is somewhat surprising in view of the approximation (B5) used in (B7) of Appendix B, which is apparently offset by (B9).

TABLE 3. COMPARISON OF GROUP PATH LENGTHS CALCUALTED FROM TWO MARTYN TYPES OF RELATIONS (cf. Sec. 4)

FREQ. (MHz)	EL. ANGLE (o)	EXACT P' (km)	PM' (km)	PR2' (km)
11	10	1984.30	1985.35	1984.30
	15	1589.92	1591.18	1589.93
	20	1336.35	1337.88	1336.35
	25	1170.83	1172.69	1170.84
	35	993.03	995.83	993.05
	45	936.40	940.98	936.45
	55	978.85	989.37	979.04
	60	1073.50	1101.61	1074.04
	61	1110.72	1152.10	1111.46
	62	1164.85	1240.87	1166.01
8	10	1938.26	1938.53	1938.26
	15	1534.97	1535.28	1534.97
	20	1270.06	1270.41	1270.06
	30	966.24	966.69	966.24
	40	813.65	814.16	813.65
	50	733.92	734.44	733.92
	60	693.75	694.20	693.76
	70	676.09	676.37	676.09
	80	670.25	670.34	670.25

Because of the high accuracy of the derived generalizations of the flat ionosphere theorems of Breit-Tuve and Martyn, these generalizations can form the basis of a highly accurate algorithm for range determination at any measured elevation angle. The algorithm is given next.

---------- ALGORITHM 2 ----------

(1) Determine the reflection radius R_t from eq. (16)
(2) From the calculations of eq's (17) - (22), determine the group path delay P' in terms of the density slope at R_t, the virtual height at the frequency f_v given by eq. (17), and some characteristics of the observed E-layer.
(3) Determine range from P' according to eq. (15), i.e.,

$$\chi_D = \frac{R_o}{R_t}\left(\frac{P'\cos\beta_o}{2R_t} + \frac{R_t}{R_o}\chi_t - \sin\chi_t\right) \qquad (23)$$

where χ_t is given by eq. (15). This algorithm is different in character from the simple algorithm of Sec. 3. Note, for example, that it is not iterative.

5. DISCUSSION

Within the approximations of constant ionosphere and no magnetic field the simple algorithm of Sec. 3 is sufficiently accurate for range determination in most cases. The only breakdown occurs at high elevation angles (cf. Table 1), in the region of Pedersen ray propagation for $f > f_p$, and this arises principally from the use Martyn's equivalent path theorem for a flat ionosphere.

Curved ionosphere generalizations of the Breit-Tuve and Martyn theorems are derived in the preceding section, and are shown to be capable of removing the inaccuracies in the algorithm of Sec. 3. Unfortunately, additional complication is introduced. Not only is the virtual height vs frequency profile required, but also the density vs. height profile in the vicinity of the reflection height must be known. The latter is required in order to be able to determine the reflection height and the slope of the density at this height. Partial knowledge of the electron density vs. height profile is the typical outcome of processing the virtual height profiles from vertical ionosonde measurements ([Titheridge, 1959] and [Budden, 1966]). For example, electron density valley values behind (above) an E-layer peak remain unknown. It is conceivable, therefore, that enough about the density profile is known that the algorithm at the end of Sec. 4 can be applied, but that not enough of the profile is known to enable application of a ray-tracing program or a direct-scattering algorithm of the type given in Sec. 2. Even when the direct scattering calculation is possible, it may well be that the algorithm of Sec. 4 is simpler to apply. This depends on the type of data and both data-handling and computing power which are available at the time.

Curved ionosphere generalizations of the Breit-Tuve and Martyn theorems may turn out to be useful in other applications too. For example, the use of (15) may enhance the accuracy of density profile extraction from oblique incidence ionograms by a method similar to that of Smith [1970]. In conjunction with such a procedure it may be that conversion of oblique incidence ionograms to virtual height profiles would be facilitated through use of (16)-(22).

The use of curved ionosphere generalizations may seem questionable when one accepts 5-10% inaccuracies from the neglect of ionospheric tilts and mangetic fields. It is only the use of Martyn's theorem for flat ionosphere at high elevation angles and frequencies ($f \gtrsim f_p$) that results in errors of this magnitude. In other cases, the use of the simple algorithm in Sec. 3 is attractive. Development of techniques in DF applications for making corrections due to the magnetic field and ionospheric tilts should justify more extensive use of the curved ionosphere generalizations of the Breit-Tuve and Martyn theorems.

Throughout this paper, attention has been principally directed to range determination in HF-DF applications. The latitude and longitude of the HF transmitter are easily found from azimuth and range by the use of simple spherical trigonometry formulae.

REFERENCES

1. Budden K.G., (1966), Radio Waves in the Ionosphere, Cambridge University Press, London

2. Croft T.A. and H. Hoogasian (1968), "Exact Ray Calculations in a Quasiparabolic Ionosphere", Radio Science 3 (new series), No. 1, p. 69-74.

3. Freehafer J.E., (1951), "Geometrical Optics", in Propagation of Short Radio Waves, ed. by D.E. Kerr, McGraw-Hill and Dover Publications (1965), New York

4. Gething P.J.D. (1978), Radio Direction Finding, Peter Peregrinus Ltd on behalf of the IEEE, England

5. Smith M.S., (1970), "The Calculation of Ionospheric Profiles from Data Given on Oblique Incidence Ionograms", J. Atmosph. and Terr. Phys. 32, pp 1047-1056.

6. Titheridge J.E., "The Calculation of Real and Virtual Heights of Reflection in the Ionosphere", J. Atmosph. and Terr. Phys., 17, pp 1047-1056, 1970

7. deVoogt A.H., "The Calculation of the Path of a Radio-Ray in a Given Ionosphere", Proc IRE 41, pp. 1183-1186, 1953.

APPENDIX A

DIRECT SCATTERING CALCULATION OF RANGE AND GROUP PATH LENGTH

Given three adjacent mesh points R_1, R_2, and R_3 with associated values of $G = R^2 f_N^{\,2}$, where f_N is the plasma frequency. A quadratic fit to G(R) on the interval $[R_1, R_3]$ is given by Lagrangian interpolation:

$$G \approx G_1 \frac{(R-R_2)(R-R_3)}{(R_1-R_2)(R_1-R_3)} + G_2 \frac{(R-R_3)(R-R_1)}{(R_2-R_3)(R_2-R_1)} + G_3 \frac{(R-R_1)(R-R_2)}{(R_3-R_1)(R_3-R_2)} \tag{A1}$$

$$= \epsilon_{ijk}\, G_i \frac{(R-R_j)(R-R_k)}{(R_i-R_j)(R_i-R_k)}$$

where ϵ_{ijk} is the familiar Levi-Centa tensor, (= 0 if any two indices are equal, otherwise = +1, -1 for an even, odd permutation of indices) and the summation from 1 to 3 is understood for repeated indices. Then in eq. (5) if the text, one can write (cf (1) of text)

$$F(R) \equiv \mu^2 R^2 - R_0^2 \cos^2\beta_0 = AR^2 + BR + C \tag{A2}$$

where

$$A = 1 - \epsilon_{ijk} \frac{G_i}{f^2(R_i-R_j)(R_i-R_k)}$$

$$B = \epsilon_{ijk} \frac{G_i (R_j+R_k)}{f^2(R_i-R_j)(R_i-R_k)} \tag{A3}$$

$$C = -\epsilon_{ijk} \frac{G_i R_j R_k}{f^2(R_i-R_j)(R_i-R_k)} - R_0^2 \cos^2\beta_0$$

With the approximation of the preceding eq's. the contribution to x from this radius interval is

$$X_i = R_0 \cos\beta_0 \int_{R_1}^{R_3} \frac{dR}{R\sqrt{AR^2+BR+C}}\,, \tag{A6}$$

which is analytically integrable. If there is a reflection point R_t in the interval, such that

$$F(R_t) \equiv A R_t^2 + B R_t + C = 0 \qquad \text{(A7)}$$

then the upper limit R_3 should be replaced by R_t. Hence, assuming the electron density is non-vanishing in the interval, it is found that

$$\chi_i = \frac{R_0 \cos\beta_0}{\sqrt{C}} \ln \left(\frac{\sqrt{F(R)} + \sqrt{C}}{R} + \frac{B}{2\sqrt{C}} \right) \Bigg|_{R_3}^{R_1} \qquad \text{(A8)}$$

From Eq. (9) of the text and (A2) above, the ionospheric contribution to group path length from the given triad of points is similarly obtained. It is

(A9)

$$P_i'/2 = \frac{1}{A} \left\{ \sqrt{F(R)} - \frac{B}{2\sqrt{A}} \ln \left(\sqrt{F(R)} + \sqrt{A}\, R + \frac{B}{2\sqrt{A}} \right) \right\} \Bigg|_{R_1}^{R_3},$$

where R_3 should be replaced by the reflection pt. R_t, if such a point exists in the interval.

APPENDIX B

GENERALIZATION OF MARTYN'S THEOREM

From equations ((1) and (9) of the text, group path length for an oblique path is given by

$$P'/2 = \int_{R_0}^{R_t} dR / \sqrt{Q(R)} \quad , \tag{B1}$$

where

$$Q(R) \equiv 1 - f_N^2(R)/f^2 - (R_0 \cos\beta_0 / R)^2 \tag{B2}$$

vanishes at R_t, the reflection radius in the F-layer. The frequency is assumed to be large enough that an E-layer present is penetrated. Let the bottom of the F-layer be located at R_{BF}. Then from (10) of the text

$$P'/2 = \sqrt{R_{BF}^2 - R_0^2\cos^2\beta_0} - R_0 \sin\beta_0 + \Delta_E(f,\beta_0) + \int_{R_{BF}}^{R_t} \frac{dR}{\sqrt{Q(R)}} \tag{B3}$$

where Δ_E is the retardatation length due to the E-layer in the region $R_{BE} \leq R \leq R_{TE}$. It is given by

$$\Delta_E(f,\beta_0) \equiv \int_{R_{BE}}^{R_{TE}} \frac{dR}{\sqrt{Q(R)}} - \left(\sqrt{R_{TE}^2 - R_0^2\cos^2\beta_0} - \sqrt{R_{BE}^2 - R_0^2\cos^2\beta_0} \right) \tag{B4}$$

The approximation is now made that for the integral in (B2), Q(R) can be replaced by an expression which is valid when R is near R_t:

$$Q(R) \approx |Q'(R_t)|\,(R_t - R) \qquad (R \leq R_t), \tag{B5}$$

where

$$Q'(R) = -\frac{1}{f^2}\frac{d f_N^2(R)}{dR} + \frac{2}{R}\left(\frac{R_0\cos\beta_0}{R}\right)^2 \tag{B6}$$

Then (B3) becomes

$$P'/2 = \sqrt{R_{BF}^2 - R_0^2\cos^2\beta_0} - R_0\sin\beta_0 + \Delta_E(f,\beta_0) + 2\sqrt{(R_t - R_{BF})/|Q'(R_t)|} \tag{B7}$$

Evidently, this expression is suspect when R_t is very close to the layer maximum. The corresponding expression for vertical incidence ($\beta_o = \pi/2$)) is

$$h'(f_v) = R_{BF} - R_o + \Delta_E(f_v, \pi/2) + 2\sqrt{(R_t - R_{BF})/|Q_v'(R_t)|} \quad , \tag{B8}$$

where

$$f_v = f\sqrt{1 - (R_o \cos\beta_o / R_t)^2}$$

is now the frequency that enters this expression, in order that reflection takes place at the same height H_t as for the oblique incidence propagation. Here, $Q_v'(R_t)$ in (B8) is given by (B6) with $\beta_o = \pi/2$ and with f replaced by f_v. Every radius R in these equations is associated with an altitude H, defined by $H = R - R_o$. It is proposed to generalize Martyn's equivalent path theorem by using (B8) to eliminate R_{BF} from (B7). In this way a new relation between $P'/2$ and $h'(f_v)$ is obtained. From (B8), the expression for H_{BF} is

$$H_{BF} = \hat{h}_v - K_v + K_v\sqrt{1 - 2(\hat{h}_v - H_t)/K_v} \quad , \tag{B9}$$

where

$$K_v \equiv 2/|Q_v'(R_t)| \tag{B10}$$

$$\hat{h}_v \equiv h'(f_v) - \Delta_E(f_v, \pi/2)$$

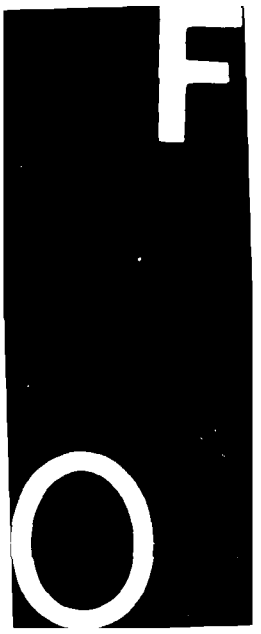
F
O